Biomech Model Mechanobiol (2016) 15:1669–1684
DOI 10.1007/s10237-016-0790-5

ORIGINAL PAPER

Stability analysis of a continuum-based constrained mixture model for vascular growth and remodeling

Jiacheng Wu[1] · **Shawn C. Shadden**[1]

Received: 8 August 2015 / Accepted: 8 April 2016 / Published online: 26 April 2016

Abstract A stabilizing criterion is derived for equations governing vascular growth and remodeling. We start from the integral state equations of the continuum-based constrained mixture theory of vascular growth and remodeling and obtain a system of time-delayed differential equations describing vascular growth. By employing an exponential form of the constituent survival function, the delayed differential equations can be reduced to a nonlinear ODE system. We demonstrate the degeneracy of the linearized system about the homeostatic state, which is a fundamental cause of the neutral stability observations reported in prior studies. Due to this degeneracy, stability conclusions for the original nonlinear system cannot be directly inferred. To resolve this problem, a sub-system is constructed by recognizing a linear relation between two states. Subsequently, Lyapunov's indirect method is used to connect stability properties between the linearized system and the original nonlinear system, to rigorously establish the neutral stability properties of the original system. In particular, this analysis leads to a stability criterion for vascular expansion in terms of growth and remodeling kinetic parameters, geometric quantities and material properties. Numerical simulations were conducted to evaluate the theoretical stability criterion under broader conditions, as well as study the influence of key parameters and physical factors on growth properties. The theoretical results are also compared with prior numerical and experimental findings in the literature.

✉ Shawn C. Shadden
shadden@berkeley.edu

Jiacheng Wu
wujiacheng@berkeley.edu

[1] Department of Mechanical Engineering, University of California, Berkeley, CA, USA

Keywords Constrained mixture theory · Growth and remodeling · Stability analysis · Blood vessel

1 Introduction

The functional adaptation of arteries to biomechanical stimuli has been long recognized as an important feature of vascular growth and remodeling (G&R) and has led to the development of mathematical theories to describe such phenomena (Humphrey 2006). A common theoretical framework has been the constrained mixture theory model for studying growth and remodeling of soft tissues (Humphrey and Rajagopal 2002). Previous research in applying the constrained mixture theory of vascular G&R has focused mostly on numerical investigations, and especially in relation to aneurysm growth. For example, Baek et al. (2005, 2006) applied the constrained mixture theory to study stress-mediated aneurysm expansion in idealized geometries to better understand different factors influencing geometry and aneurysm growth rate. Later, G&R theory was extended to 3D geometries to predict complex aneurysm shapes (Zeinali-Davarani et al. 2011). In addition, vascular G&R simulations have been coupled with blood flow dynamics to study the coupling between hemodynamics (e.g., wall shear stress) and vascular adaptations in cylindrical-type geometries (Figueroa et al. 2009; Watton et al. 2009; Sheidaei et al. 2011) and more recently to patient-specific geometries (Wu and Shadden 2015).

It has been suggested (Bogen and McMahon 1979; Austin et al. 1989) that a better understanding for risk of aneurysm rupture may involve the stability of aneurysm expansion due to vascular G&R, i.e., rupture might be a result of unstable vascular G&R. While the above studies considered the numerical implementation of G&R in various applications,

theoretical analysis of the stability of the underlying adaptive mechanism has received less attention. In this regard, the recent work of Satha et al. (2014) studied the arterial growth instability using a goal function-based approach. In important work of Cyron and Humphrey (2014), Cyron et al. (2014), the authors introduced the concept of mechanobiological stability based on comprehensive analysis of the differential equations of mass density and vessel wall position from vascular G&R theory. As shown herein, the mathematical underpinnings of mechanobiological stability can be seen to have origins in the degenerate nature of the (linearized) system about the homeostatic state. This degeneracy complicates the use of linear stability analysis to study the stability of the homeostatic state to infer the stability of the original (nonlinear) system. In this work, we start from the integral state equations of the continuum-based constrained mixture model of G&R and derive the state equations (time-delayed differential equations) describing vascular expansion. By employing a commonly used exponential form of the constituent survival function and by introducing an extended state variable, the delayed differential equations can be reduced to an ODE system. Linear stability analysis is subsequently applied to this ODE system, and a stability criterion is obtained based on G&R kinetic parameters and material properties. To address the problem of the degeneracy of the linearized system about the homeostatic state mentioned above, we formulate a reduced sub-system that is shown to be exponentially stable, which enables us to extend the linear stability results to the original (nonlinear) system and rigorously prove stability properties observed in prior computational and theoretical studies.

2 Constrained mixture theory of growth and remodeling

The vessel wall has the ability to adapt to changes of mechanical environment to maintain a homeostatic state via vascular G&R (Humphrey 2006; Valentin and Humphrey 2009). This process occurs through removal of old vascular constituents and incorporation of new constituents, which can be described by an equation of the form

$$M(t) = M(0)Q(t) + \int_0^t m(\tau)q(t-\tau)\mathrm{d}\tau. \tag{1}$$

$M(t)$ is the mass per unit area of vascular constituents at time t. The first term on the right represents the contribution from the "initial" mass before G&R, whereas the second term on the right represents the incorporation and natural turnover of newly produced constituent. Specifically, $Q(t)$ is the remaining fraction of initial mass at the current time t, $m(\tau)$ is the mass production rate of vascular constituent at time τ, and $q(t-\tau)$ is the remaining fraction of newly produced constituent at time t.

The mass production rate $m(t)$ is assumed to depend linearly on the deviation of wall tension σ with respect to a homeostatic stress σ_h (Baek et al. 2006),

$$m(t) = M(t)\left[k_\mathrm{g}[\sigma(t) - \sigma_\mathrm{h}] + f_\mathrm{h}\right] \tag{2}$$

where k_g is the growth feedback constant and f_h is the basal value of the mass production rate. The above growth law describes the stress-mediated feedback mechanism by which the homeostatic stress is maintained.

In the constrained mixture theory of G&R (Humphrey and Rajagopal 2002), the vessel wall is modeled as a membrane and treated as a constrained mixture, i.e., all vascular constituents deform together at each location. The reference configuration κ_0 for the vascular mixture corresponds to the configuration with zero transmural pressure. For any time t, the current configuration of the mixture is denoted as $\kappa(t)$, and $\mathbf{F}(t)$ is the deformation gradient tensor mapping from κ_0 to $\kappa(t)$. However, the deformation of individual vascular constituents is computed with respect to their natural configurations $\kappa_{n(\tau)}$, which depends on the time τ when the constituent was produced. The newly produced vascular constituent is deposited into the vascular mixture with pre-stretch defined by $\mathbf{G}(\tau)$, which maps from the natural configuration $\kappa_{n(\tau)}$ to the deformed configuration of the mixture at τ. Therefore, based on the relations between different configurations shown in Fig. 1, the deformation gradient tensor of the vascular constituents produced at time τ mapping from the natural configuration $\kappa_{n(\tau)}$ to the current deformed configuration $\kappa(t)$ is defined as

$$\mathbf{F}_{n(\tau)}(t) = \mathbf{F}(t)\mathbf{F}^{-1}(\tau)\mathbf{G}(\tau). \tag{3}$$

The right Cauchy–Green deformation tensor is computed as

$$\mathbf{C}_{n(\tau)}(t) = \mathbf{F}_{n(\tau)}(t)^T\mathbf{F}_{n(\tau)}(t). \tag{4}$$

The pre-stretch tensor $\mathbf{G}(\tau)$ is defined as the two-point tensor

$$\mathbf{G}(\tau) = G_\mathrm{h}\mathbf{e}(\tau) \otimes \mathbf{e}_{n(\tau)}, \tag{5}$$

where $\mathbf{e}(\tau)$ is the direction of vascular constituent at time τ in the mixture configuration $\kappa(\tau)$ and $\mathbf{e}_{n(\tau)}$ is the direction of the vascular constituent produced at time τ in its natural configuration $\kappa_{n(\tau)}$. The relation between $\mathbf{e}(\tau)$ and $\mathbf{e}_{n(\tau)}$ is described by

$$\mathbf{e}_{n(\tau)} = \frac{\mathbf{G}(\tau)^{-1}\mathbf{e}(\tau)}{\left\|\mathbf{G}(\tau)^{-1}\mathbf{e}(\tau)\right\|}. \tag{6}$$

G_h is the pre-stretch of the vascular constituent when it is deposited into the mixture, and since we assume it is equal

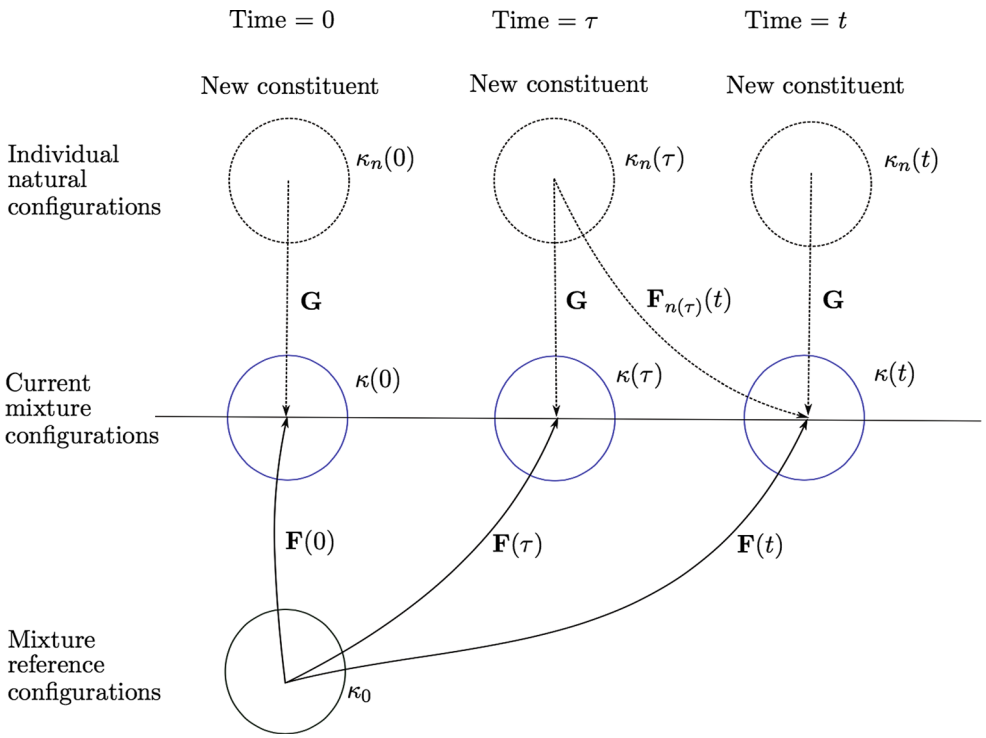

Fig. 1 Configurations and associated mappings used to describe G&R framework

to the stretch ratio of vascular constituent in the homeostatic state, we mark it using the subscript "h".

After $\mathbf{C}_{n(\tau)}(t)$, $\mathbf{G}(\tau)$ and $\mathbf{e}_{n(\tau)}$ are defined, the stretch ratio of the vascular constituent produced at time τ with respect to its natural configuration $\kappa_{n(\tau)}$ can be computed as

$$\begin{aligned}\lambda_{n(\tau)}(t) &= \sqrt{\mathbf{e}_{n(\tau)} \cdot \mathbf{C}_{n(\tau)}(t)\mathbf{e}_{n(\tau)}} \\ &= \left\|\mathbf{F}(t)\mathbf{F}^{-1}(\tau)\mathbf{G}(\tau)\mathbf{e}_{n(\tau)}\right\| \\ &= \left\|\mathbf{F}(t)\mathbf{F}^{-1}(\tau)G_{\mathrm{h}}\left(\mathbf{e}(\tau)\otimes\mathbf{e}_{n(\tau)}\right)\mathbf{e}_{n(\tau)}\right\| \\ &= G_{\mathrm{h}}\left\|\mathbf{F}(t)\mathbf{F}^{-1}(\tau)\mathbf{e}(\tau)\right\| \\ &= G_{\mathrm{h}}\frac{\left\|\mathbf{F}(t)\mathbf{F}^{-1}(\tau)\mathbf{e}(\tau)\right\| / \left\|\mathbf{F}^{-1}(\tau)\mathbf{e}(\tau)\right\|}{\|\mathbf{e}(\tau)\| / \left\|\mathbf{F}^{-1}(\tau)\mathbf{e}(\tau)\right\|} \\ &= G_{\mathrm{h}}\frac{\lambda(t)}{\lambda(\tau)},\end{aligned} \tag{7}$$

where $\lambda(t)$ is the stretch ratio of the mixture in the direction of the vascular constituent, defined as

$$\lambda(t) = \frac{\left\|\mathbf{F}(t)\mathbf{F}^{-1}(\tau)\mathbf{e}(\tau)\right\|}{\left\|\mathbf{F}^{-1}(\tau)\mathbf{e}(\tau)\right\|}. \tag{8}$$

Based on the mass-averaged principle for a constrained mixture, the total strain energy per unit area for the mixture at current time t is

$$\begin{aligned}W(t) = &\frac{M(0)}{\rho}Q(t)\hat{W}(\lambda_{n(0)}(t)) \\ &+ \int_0^t \frac{m(\tau)}{\rho}q(t-\tau)\hat{W}(\lambda_{n(\tau)}(t))\mathrm{d}\tau,\end{aligned} \tag{9}$$

where ρ is the volume density of the vessel wall and $\hat{W}$ denotes the strain energy per unit volume, which depends on the stretch ratio $\lambda_{n(\tau)}(t)$. The mathematical form of $\hat{W}$ is determined by the constitutive relation.

Our goal is to perform stability analysis of vascular G&R. To simplify the analysis while retaining the essential dynamics, we assume the geometry is cylindrical and deformation occurs in the radial direction. For conciseness of exposition, we assume here that vascular constituents are aligned in the circumferential direction. We later in Sect. 4.7, discuss the extension of this model to the case of multiple vascular constituent orientations, which is known to occur in vivo.

Under these assumptions, the stretch ratio of the mixture in the circumferential direction, $\lambda_{\mathrm{circ}}(t)$, is obtained as

$$\lambda_{\mathrm{circ}}(t) = \frac{\left\|\mathbf{F}(t)\mathbf{F}^{-1}(\tau)\mathbf{e}_{\mathrm{circ}}\right\|}{\left\|\mathbf{F}^{-1}(\tau)\mathbf{e}_{\mathrm{circ}}\right\|} = \frac{r(t)}{R}, \tag{10}$$

where $r(t)$ is the vessel radius at time t in the mixture configuration $\kappa(t)$ and R is the vessel radius in the mixture reference configuration κ_0. Hence, the stretch ratio of the vascular constituents with respect to the natural configuration is obtained as

$$\lambda_{n(\tau)}(t) = G_{\mathrm{h}} \frac{\lambda_{\mathrm{circ}}(t)}{\lambda_{\mathrm{circ}}(\tau)} = G_{\mathrm{h}} \frac{r(t)}{r(\tau)}. \tag{11}$$

For conciseness of exposition, we here assume a linearized stress–strain relation with respect to the homeostatic states of the vessel wall for the purpose of stability analysis. However, since vascular material is usually considered nonlinear (Holzapfel et al. 2000; Humphrey 2013), we later in Sect. 4.6 discuss the extension of the model for a nonlinear material model. Based on the above assumptions,

$$\begin{aligned}\hat{W}(\lambda_{n(\tau)}(t)) &= \frac{1}{2} E \left[\lambda_{n(\tau)}(t) - 1\right]^2 \\ &= \frac{1}{2} E \left[G_{\mathrm{h}} \frac{r(t)}{r(\tau)} - 1\right]^2,\end{aligned} \tag{12}$$

where $\lambda_{n(\tau)}(t) - 1$ represents the strain of the vascular constituents with respect to their natural configurations $\kappa_{n(\tau)}$. Therefore, (9) becomes

$$\begin{aligned}W(t) = &\frac{M(0)}{\rho} Q(t) \frac{1}{2} E \left[G_{\mathrm{h}} \frac{r(t)}{r_{\mathrm{h}}} - 1\right]^2 \\ &+ \int_0^t \frac{m(\tau)}{\rho} q(t-\tau) \frac{1}{2} E \left[G_{\mathrm{h}} \frac{r(t)}{r(\tau)} - 1\right]^2 \mathrm{d}\tau,\end{aligned} \tag{13}$$

where r_{h} is initial homeostatic value for vessel radius. Note that for the initial mass, the stretch ratio is equal to $G_{\mathrm{h}} \frac{r(t)}{r_{\mathrm{h}}}$ instead of $G_{\mathrm{h}} \frac{r(t)}{r(0)}$ because the initial vascular constituents are not necessarily produced at $t = 0$. Instead, they are produced when the vessel radius equals to r_{h} since we assumed the tissue is in the homeostatic state before $t = 0$, after which point G&R occurs.

We are here interested in system stability and hence the long-term behavior of the model. Due to natural turnover, the "initial" mass terms in both (1) and (13) decay to zero in time upon integration of the differential equations. Thus, in terms of stability analysis, we are left with

$$M(t) = \int_0^t m(\tau) q(t-\tau) \mathrm{d}\tau \tag{14}$$

$$W(t) = \int_0^t \frac{m(\tau)}{\rho} q(t-\tau) \frac{1}{2} E \left[G_{\mathrm{h}} \frac{r(t)}{r(\tau)} - 1\right]^2 \mathrm{d}\tau. \tag{15}$$

This simplification is for analytical convenience; we show in the Results section that the initial mass values, which are required for numerical simulations, do not affect stability conclusions. In the case of cylindrical geometry, the force balance equation in the circumferential direction yields

$$Pr(t) = T_\theta(t) = \frac{1}{\lambda_z(t)} \frac{\partial W(t)}{\partial \lambda_\theta(t)}, \tag{16}$$

where

$$\lambda_z = 1, \quad \lambda_\theta(t) = \frac{r(t)}{R}. \tag{17}$$

Therefore,

$$\begin{aligned}\frac{\partial W(t)}{\partial \lambda_\theta} &= R \frac{\partial W(t)}{\partial r(t)} \\ &= R \int_0^t \frac{m(\tau)}{\rho} q(t-\tau) \\ &\quad \times E \left[G_{\mathrm{h}} \frac{r(t)}{r(\tau)} - 1\right] \frac{G_{\mathrm{h}}}{r(\tau)} \mathrm{d}\tau.\end{aligned} \tag{18}$$

Substituting the above into (16) yields

$$\begin{aligned}Pr(t) = R &\int_0^t \frac{m(\tau)}{\rho} q(t-\tau) \\ &\times E \left[G_{\mathrm{h}} \frac{r(t)}{r(\tau)} - 1\right] \frac{G_{\mathrm{h}}}{r(\tau)} \mathrm{d}\tau.\end{aligned} \tag{19}$$

Note that mean arterial pressure is used here and is assume to be constant. Although pressure varies over the cardiac cycle, we assume mean pressure is of most interest in the long-term behavior of vascular G&R.

3 Converting to an ODE system

From the previous section, the time evolution of vascular growth and remodeling is described by the following equations

$$M(t) = \int_0^t m(\tau) q(t-\tau) \mathrm{d}\tau, \tag{20}$$

$$\begin{aligned}Pr(t) = R &\int_0^t \frac{m(\tau)}{\rho} q(t-\tau) \\ &\times E \left[G_{\mathrm{h}} \frac{r(t)}{r(\tau)} - 1\right] \frac{G_{\mathrm{h}}}{r(\tau)} \mathrm{d}\tau,\end{aligned} \tag{21}$$

$$m(t) = M(t) \left[k_{\mathrm{g}}[\sigma(t) - \sigma_{\mathrm{h}}] + f_{\mathrm{h}}\right], \tag{22}$$

$$\sigma(t) = \frac{Pr(t)}{h(t)}, \tag{23}$$

where $h(t) = \frac{M(t)}{\rho J(t)}$ is the vessel wall thickness and J is the determinant of the deformation gradient tensor, which is equal to $\frac{r(t)}{R}$. Since the current behavior of the system depends continuously on all past time history, the system is a continuous time-delayed system. For analysis, it is convenient if we can convert this to an ODE system depending on current states. To make this reduction possible, we assume the survival function has an exponential decay

$$q(t) = \exp(-\alpha t), \tag{24}$$

where $\alpha > 0$ is the decay constant. This implies that the rate of decay of the constituent is proportional to its current value as

$$\dot{q}(t) = -\alpha q(t). \tag{25}$$

To proceed, we differentiate (20) with respect to t

$$\dot{M}(t) = m(t) - \alpha \int_0^t m(\tau) q(t-\tau) \mathrm{d}\tau \tag{26}$$

$$= m(t) - \alpha M(t). \tag{27}$$

Substituting in (22) yields

$$\dot{M}(t) = M(t) k_{\mathrm{g}} \left[\sigma(t) - \sigma_{\mathrm{h}}\right] + M(t) \left[f_{\mathrm{h}} - \alpha\right]. \tag{28}$$

Since f_{h} is the basal value of the mass production rate, it should balance with the natural decay of constituents caused by the survival function $q(t)$. Thus, we require that $f_{\mathrm{h}} = \alpha$ and subsequently

$$\dot{M}(t) = M(t) k_{\mathrm{g}} \left[\sigma(t) - \sigma_{\mathrm{h}}\right]. \tag{29}$$

Now taking the time derivative of (21) yields

$$\begin{aligned} P\dot{r}(t) = R \Bigg[& \frac{m(t)}{\rho} E \left(G_{\mathrm{h}} - 1\right) \frac{G_{\mathrm{h}}}{r(t)} \\ & + \int_0^t \frac{m(\tau)}{\rho} q(t-\tau) E \, G_{\mathrm{h}} \frac{\dot{r}(t)}{r(\tau)} \frac{G_{\mathrm{h}}}{r(\tau)} \mathrm{d}\tau \\ & - \alpha \int_0^t \frac{m(\tau)}{\rho} q(t-\tau) \\ & \times E \left[G_{\mathrm{h}} \frac{r(t)}{r(\tau)} - 1 \right] \frac{G_{\mathrm{h}}}{r(\tau)} \mathrm{d}\tau \Bigg]. \end{aligned} \tag{30}$$

The last term in the above equation is just $-\alpha P r(t)$, and defining an extended state variable

$$y(t) = R \int_0^t \frac{m(\tau)}{\rho} q(t-\tau) E \frac{G_{\mathrm{h}}^2}{r^2(\tau)} \mathrm{d}\tau \tag{31}$$

yields

$$\dot{r}(t) = \frac{m(t)}{r(t)} \frac{RE\left[G_{\mathrm{h}} - 1\right] G_{\mathrm{h}}}{P\rho} + \frac{1}{P} y(t) \dot{r}(t) - \alpha r(t). \tag{32}$$

Taking the time derivative of (31), we obtain the ODE characterizing dynamics of $y(t)$

$$\dot{y}(t) = k_2 \frac{m(t)}{r^2(t)} - \alpha y(t), \tag{33}$$

where $k_2 = \frac{G_{\mathrm{h}}^2 ER}{\rho}$. The extended state y represents the generalized stiffness of the vascular mixture, as explained later in Sect. 6.

Based on (22), (23), (29), (32) and (33), the system of equations for vascular growth can now be written as

$$\dot{M}(t) = M(t) k_{\mathrm{g}} \left[\sigma(t) - \sigma_{\mathrm{h}}\right] \tag{34}$$

$$\dot{r}(t) = \frac{1}{k(t)} \left[\alpha r(t) - \frac{m(t)}{r(t)} k_1 \right] \tag{35}$$

$$\dot{y}(t) = k_2 \frac{m(t)}{r^2(t)} - \alpha y(t) \tag{36}$$

$$m(t) = M(t) \left[k_{\mathrm{g}} \left[\sigma(t) - \sigma_{\mathrm{h}}\right] + f_{\mathrm{h}} \right] \tag{37}$$

$$\sigma(t) = \frac{\rho P r(t)^2}{M(t) R} \tag{38}$$

where $k(t) = \frac{1}{P} y(t) - 1$, $k_1 = \frac{RE[G_{\mathrm{h}}-1]G_{\mathrm{h}}}{P\rho}$ and $f_{\mathrm{h}} = \alpha$.

4 Stability analysis of the ODE system

4.1 Linearization of state equations

The stability of vascular growth is characterized by the stability of the ODE system we obtained in previous section. To analyze its stability, we examine the nature of the linearized system about the homeostatic state. Namely, we assume the vessel is initially in its homeostatic state before G&R is introduced by whatever cause. Mass density and vessel radius in the initial homeostatic state are denoted M_{h} and r_{h}, respectively. Strictly speaking, as shown later, there is no "homeostatic state" for mass density $M(t)$ and $r(t)$ because asymptotic stability does not hold for $M(t)$ and $r(t)$. However, for convenience, we use the term "homeostatic state" to denote the asymptotic values M_{h} and r_{h}.

Based on (38), the homeostatic value of circumferential stress σ_{h} is

$$\sigma_{\mathrm{h}} = \frac{\rho P r_{\mathrm{h}}^2}{M_{\mathrm{h}} R}. \tag{39}$$

Substituting homeostatic values into (32) yields

$$\frac{\rho P r_{\mathrm{h}}}{M_{\mathrm{h}}} = E\left[G_{\mathrm{h}} - 1\right]. \tag{40}$$

Combining (39) and (40) and observing $G_{\mathrm{h}} = \frac{r_{\mathrm{h}}}{R}$, we obtain an alternate expression for σ_{h}

$$\sigma_{\mathrm{h}} = E\left[G_{\mathrm{h}} - 1\right] G_{\mathrm{h}}. \tag{41}$$

Similarly, substituting homeostatic values into (31) yields the homeostatic value for the extended state $y(t)$

$$y_{\mathrm{h}} = \frac{RE G_{\mathrm{h}}^2 M_{\mathrm{h}}}{\rho r_{\mathrm{h}}^2}. \tag{42}$$

We next consider perturbation of the system around the homeostatic values above

$$M(t) = M_\mathrm{h} + \Delta M(t) \tag{43}$$
$$r(t) = r_\mathrm{h} + \Delta r(t) \tag{44}$$
$$y(t) = y_\mathrm{h} + \Delta y(t) \tag{45}$$
$$\sigma(t) = \sigma_\mathrm{h} + \Delta\sigma(t) \tag{46}$$

with

$$\frac{\Delta M}{M_\mathrm{h}}, \ \frac{\Delta r}{r_\mathrm{h}}, \ \frac{\Delta y}{y_\mathrm{h}}, \ \frac{\Delta\sigma}{\sigma_\mathrm{h}} \ll 1. \tag{47}$$

To obtain the linearized equations, it is convenient to first obtain the first-order approximation of $\Delta\sigma$

$$\begin{aligned}\Delta\sigma(t) &= \sigma(t) - \sigma_\mathrm{h} \\ &= \frac{\rho P}{R}\left[\frac{[r_\mathrm{h}+\Delta r]^2}{M_\mathrm{h}+\Delta M} - \frac{r_\mathrm{h}^2}{M_\mathrm{h}}\right] \\ &\approx \frac{\rho P}{R}\left[\frac{2r_\mathrm{h}}{M_\mathrm{h}}\Delta r - \frac{r_\mathrm{h}^2}{M_\mathrm{h}^2}\Delta M\right].\end{aligned} \tag{48}$$

Therefore, the linearized state equation for mass density $M(t)$ is obtained as

$$\begin{aligned}\Delta\dot{M} = \dot{M} &= M k_\mathrm{g}\Delta\sigma \\ &\approx [M_\mathrm{h}+\Delta M]k_\mathrm{g}\frac{\rho P}{R}\left[\frac{2r_\mathrm{h}}{M_\mathrm{h}}\Delta r - \frac{r_\mathrm{h}^2}{M_\mathrm{h}^2}\Delta M\right] \\ &\approx k_\mathrm{g}\frac{\rho P}{R}\left[2r_\mathrm{h}\Delta r - \frac{r_\mathrm{h}^2}{M_\mathrm{h}}\Delta M\right].\end{aligned} \tag{49}$$

Similarly, we can obtain the linearized state equations for vessel radius $r(t)$ and generalized stiffness $y(t)$ as

$$\begin{aligned}\Delta\dot{r} \approx \frac{1}{k_\mathrm{h}}&\left[\left[2\alpha - \frac{2k_\mathrm{g}r_\mathrm{h}^2\rho P}{RM_\mathrm{h}}\right]\Delta r\right. \\ &\left.+\left[-\frac{\alpha r_\mathrm{h}}{M_\mathrm{h}} + \frac{k_\mathrm{g}r_\mathrm{h}^3\rho P}{M_\mathrm{h}^2 R}\right]\Delta M\right]\end{aligned} \tag{50}$$

$$\begin{aligned}\Delta\dot{y} \approx &-\frac{2k_2 M_\mathrm{h}}{r_\mathrm{h}^3}\left[\alpha - \frac{k_\mathrm{g}\rho P r_\mathrm{h}^2}{RM_\mathrm{h}}\right]\Delta r \\ &-\frac{k_2}{r_\mathrm{h}^2}\left[\alpha - \frac{k_\mathrm{g}\rho P r_\mathrm{h}^2}{RM_\mathrm{h}}\right]\Delta M - \alpha\Delta y\end{aligned} \tag{51}$$

where $k_\mathrm{h} = \frac{1}{G_\mathrm{h}-1}$ and $k_2 = \frac{G_\mathrm{h}^2 ER}{\rho}$.

Equations (49)–(51) describe the time evolution of the linearized variables $(\Delta M, \Delta r, \Delta y)$. We will first consider the linear stability of the subsystem for $(\Delta M, \Delta r)$. This is reasonable since the dynamics of Δr and ΔM are decoupled from the dynamics of Δy. Also, the time evolution of mass density M and vessel radius r is of paramount interest.

Based on (49) and (50), the linearized state equations for Δr and ΔM become

$$\begin{bmatrix}\Delta\dot{r} \\ \Delta\dot{M}\end{bmatrix} = \begin{bmatrix}A & B \\ C & D\end{bmatrix} \times \begin{bmatrix}\Delta r \\ \Delta M\end{bmatrix} \tag{52}$$

where

$$A = \frac{1}{k_\mathrm{h}}\left[2\alpha - \frac{2k_\mathrm{g}r_\mathrm{h}^2\rho P}{RM_\mathrm{h}}\right], \tag{53}$$
$$B = \frac{1}{k_\mathrm{h}}\left[-\frac{\alpha r_\mathrm{h}}{M_\mathrm{h}} + \frac{k_\mathrm{g}r_\mathrm{h}^3\rho P}{M_\mathrm{h}^2 R}\right], \tag{54}$$
$$C = \frac{2k_\mathrm{g}\rho P r_\mathrm{h}}{R}, \tag{55}$$
$$D = -\frac{k_\mathrm{g}\rho P r_\mathrm{h}^2}{RM_\mathrm{h}}. \tag{56}$$

4.2 Stability of the linearized state equations

To determine whether G&R is stable, we need to first find the eigenvalues of system matrix. Let the characteristic polynomial for the system be equal to zero

$$\begin{vmatrix}A-\lambda & B \\ C & D-\lambda\end{vmatrix} = \lambda^2 - [A+D]\lambda + [AD-BC] = 0. \tag{57}$$

It can be verified that $AD - BC = 0$ based on (53)–(56). Therefore, the corresponding eigenvalues are

$$\lambda_1 = A + D, \quad \lambda_2 = 0. \tag{58}$$

This means $[\Delta r, \Delta M] = [0, 0]$ is a **degenerate** fixed point of the linearized system.

Theorem 1 (Neutrally Stable Fixed Point) *Consider an autonomous dynamical system* $\dot{\mathbf{x}} = \mathbf{A}\mathbf{x}$ *with system matrix*

$$\mathbf{A} = \begin{bmatrix}A & B \\ C & D\end{bmatrix} \tag{59}$$

whose eigenvalues are λ_1 *and* λ_2. *Let* $\tau = \mathrm{Tr}(\mathbf{A}) = A + D$, $\Delta = \det(\mathbf{A}) = AD - BC$. *If*

$$\Delta = 0, \quad \tau < 0 \tag{60}$$

then $\lambda_1 < 0$ *and* $\lambda_2 = 0$ *and there exists a line of neutrally stable non-isolated* **degenerate** *fixed points passing through* $\mathbf{x} = \mathbf{0}$. *A neutrally stable fixed point denotes a fixed point which is Lyapunov stable but not attracting.*

Based on Theorem 1, the neutrally stabilizing condition for the linearized system (52) at the fixed point $(\Delta r, \Delta M) = (0, 0)$ is $A + D < 0$, i.e.,

$$k_{\mathrm{g}} > \frac{\alpha R M_{\mathrm{h}}}{\rho P r_{\mathrm{h}}^2}\left[\frac{1}{1+\frac{E M_{\mathrm{h}}}{2\rho P r_{\mathrm{h}}}}\right]. \tag{61}$$

However, since the fixed point is degenerate, stability of the hemostatic state for the nonlinear system cannot be inferred (Verhulst 1996).

4.3 Avoiding the degeneracy condition

In order to avoid the degenerate fixed point problem encountered above, the three-state linearized system is reconsidered

$$\frac{\mathrm{d}}{\mathrm{d}t}\begin{bmatrix}\Delta r\\ \Delta M\\ \Delta y\end{bmatrix} = \begin{bmatrix} \frac{1}{k_{\mathrm{h}}}\left[\alpha - \frac{k_{\mathrm{g}}\rho P r_{\mathrm{h}}^2}{R M_{\mathrm{h}}}\right]\left[2\Delta r - \frac{r_{\mathrm{h}}}{M_{\mathrm{h}}}\Delta M\right] \\ \frac{k_{\mathrm{g}}\rho P r_{\mathrm{h}}}{R}\left[2\Delta r - \frac{r_{\mathrm{h}}}{M_{\mathrm{h}}}\Delta M\right] \\ -\frac{k_2 M_{\mathrm{h}}}{r_{\mathrm{h}}^3}\left[\alpha - \frac{k_{\mathrm{g}}\rho P r_{\mathrm{h}}^2}{R M_{\mathrm{h}}}\right]\left[2\Delta r - \frac{r_{\mathrm{h}}}{M_{\mathrm{h}}}\Delta M\right] - \alpha\Delta y \end{bmatrix}. \tag{62}$$

It can be observed that there is a linear relation between derivatives of Δr and ΔM,

$$\dot{\Delta r} = B_1 \dot{\Delta M} \tag{63}$$

where

$$B_1 = \frac{\left[\alpha - \frac{k_{\mathrm{g}}\rho P r_{\mathrm{h}}^2}{R M_{\mathrm{h}}}\right] R}{k_{\mathrm{h}} k_{\mathrm{g}} \rho P r_{\mathrm{h}}}, \tag{64}$$

which in fact is responsible for the degeneracy observed above. Note that B_1 is positive if

$$k_{\mathrm{g}} < \frac{\alpha R M_{\mathrm{h}}}{\rho P r_{\mathrm{h}}^2}. \tag{65}$$

We can now integrate the derivative relation (63) from 0 to t to obtain

$$\Delta r(t) = B_1 \Delta M(t) + B_2, \tag{66}$$

where constant B_2 only depends on initial conditions

$$B_2 = \Delta r(0) - B_1 \Delta M(0). \tag{67}$$

By eliminating Δr using the relations above, the three-state system $(\Delta r, \Delta M, \Delta y)$ is reduced to a two-state system of $(\Delta M, \Delta y)$

$$\frac{\mathrm{d}}{\mathrm{d}t}\begin{bmatrix}\Delta M\\ \Delta y\end{bmatrix} = \begin{bmatrix} \frac{k_{\mathrm{g}}\rho P r_{\mathrm{h}}}{R}\left[2B_1 - \frac{r_{\mathrm{h}}}{M_{\mathrm{h}}}\right]\Delta M + \frac{2k_{\mathrm{g}}\rho P r_{\mathrm{h}}}{R}B_2 \\ B_3 \dot{\Delta M} - \alpha \Delta y \end{bmatrix}, \tag{68}$$

where the constant B_3 is defined as

$$B_3 = -\frac{k_2\left[\alpha - \frac{k_{\mathrm{g}}\rho P r_{\mathrm{h}}^2}{R M_{\mathrm{h}}}\right] M_{\mathrm{h}} R}{k_{\mathrm{g}}\rho P r_{\mathrm{h}}^2}. \tag{69}$$

The linear system (68) is nonhomogeneous because of the constant term $\frac{2k_{\mathrm{g}}\rho P r_{\mathrm{h}}}{R}B_2$ on the right-hand side of the first equation. It can be shown that the above nonhomogeneous system is neutrally stable in the sense that the state variables $(\Delta M, \Delta y)$ remain bounded, while exponential stability cannot be obtained due to the nonhomogeneous term. However, in order to extend the stability conclusion from the linearized system to the original nonlinear system, exponential stability of the linearized system should be obtained. Therefore, we homogenize the linear system by taking the time derivative of the first equation in (68), yielding a homogeneous two-state system for $(\dot{\Delta M}, \Delta y)$ as

$$\frac{\mathrm{d}}{\mathrm{d}t}\begin{bmatrix}\dot{\Delta M}\\ \Delta y\end{bmatrix} = \begin{bmatrix} \frac{k_{\mathrm{g}}\rho P r_{\mathrm{h}}}{R}\left[2B_1 - \frac{r_{\mathrm{h}}}{M_{\mathrm{h}}}\right] & 0 \\ B_3 & -\alpha \end{bmatrix} \times \begin{bmatrix}\dot{\Delta M}\\ \Delta y\end{bmatrix}. \tag{70}$$

The eigenvalues for the system matrix in (70) are

$$\lambda_1 = \frac{k_{\mathrm{g}}\rho P r_{\mathrm{h}}}{R}\left[2B_1 - \frac{r_{\mathrm{h}}}{M_{\mathrm{h}}}\right], \quad \lambda_2 = -\alpha. \tag{71}$$

Therefore, the linear system is exponentially stable if and only if

$$\frac{k_{\mathrm{g}}\rho P r_{\mathrm{h}}}{R}\left[2B_1 - \frac{r_{\mathrm{h}}}{M_{\mathrm{h}}}\right] < 0, \quad \alpha > 0 \tag{72}$$

By substituting (64) in to the inequalities above, the exponentially stability condition is given by

$$k_{\mathrm{g}} > \frac{\alpha R M_{\mathrm{h}}}{\rho P r_{\mathrm{h}}^2}\left[\frac{1}{1+\frac{E M_{\mathrm{h}}}{2\rho P r_{\mathrm{h}}}}\right] \triangleq k_{\mathrm{cr}}, \quad \alpha > 0, \tag{73}$$

where k_{cr} denotes the critical value for the growth feedback constant k_{g} to ensure stability.

Theorem 2 (Lyapunov's Indirect Method) *Consider an autonomous nonlinear system* $\dot{\mathbf{x}} = \mathbf{f}(\mathbf{x})$ *with linearized system about* $\mathbf{x} = \mathbf{0}$ *(without loss of generality) as* $\dot{\mathbf{x}} = \mathbf{A}\mathbf{x}$*, where*

$$\mathbf{A} = \nabla \mathbf{f}(\mathbf{x})|_{\mathbf{x}=\mathbf{0}} \tag{74}$$

is the system matrix for the linear system. If the eigenvalues of matrix A satisfy

$$Re(\lambda_i) < 0, \quad \forall\, i = 1, 2, \ldots, \tag{75}$$

(i.e., the linearized system is exponentially stable), then the nonlinear system $\dot{\mathbf{x}} = \mathbf{f}(\mathbf{x})$ *is locally exponentially stable about* $\mathbf{x} = \mathbf{0}$.

Based on Theorem 2, for the nonlinear system (34)–(38) describing vascular growth, the two-state system $(\Delta\dot{M}, \Delta y)$ is locally exponentially stable, i.e., locally $\dot{M} \to 0$ and $y \to y_\mathrm{h}$ exponentially.

It can be noted that the stabilizing condition (73) for $(\Delta\dot{M}, \Delta y)$ is the same as the one in (61) derived from the degenerate linear system for $(\Delta M, \Delta r)$. (The additional criterion $\alpha > 0$ from considering Δy is automatically satisfied by definition.) However, the above analysis is necessary to establish *exponential stability* for the linear system, which enables the extrapolation of the stability properties to the original nonlinear system. On the other hand, we would like to establish the behavior of the mass density M, as opposed to its time derivative $\dot{M}$. This can be achieved, however, by noticing that, due to local exponential stability of $\Delta\dot{M}$, there exist constants $a > 0$ and $b > 0$ such that

$$\|\Delta\dot{M}\| \le be^{-at}, \quad \forall\, t > 0 \tag{76}$$

within a local neighborhood. To obtain a norm estimation of mass density $M(t)$, we first integrate $\Delta\dot{M}$ from 0 to t

$$\Delta M(t) = \Delta M(0) + \int_0^t \Delta\dot{M}\mathrm{d}t. \tag{77}$$

Taking the norm for the above equation and applying the triangle inequality gives

$$\begin{aligned}\|\Delta M(t)\| &\le \|\Delta M(0)\| + \int_0^t \|\Delta\dot{M}\|\mathrm{d}t \\ &\le \|\Delta M(0)\| + b\int_0^t e^{-at}\mathrm{d}t \\ &= \|\Delta M(0)\| + b\,\frac{1-e^{-at}}{a} \\ &\le \|\Delta M(0)\| + \frac{b}{a}.\end{aligned} \tag{78}$$

Reapplying the triangle inequality, an estimation of the norm of $M(t)$ for the nonlinear system can be obtained as

$$\begin{aligned}\|M(t)\| &= \|M_\mathrm{h} + \Delta M(t)\| \\ &\le \|M_\mathrm{h}\| + \|\Delta M(t)\| \\ &\le \|M_\mathrm{h}\| + \|\Delta M(0)\| + \frac{b}{a} \le C \\ &< \infty.\end{aligned} \tag{79}$$

Similarly, if we construct the two-state system of $(\Delta\dot{r}, \Delta y)$ and apply the same analysis above, we can obtain

$$\|r(t)\| < \infty \tag{80}$$

under the same stabilizing condition given by (73).

4.4 Asymptotic stability for wall tension $\sigma(t)$

By taking the time derivative of (38), we can obtain the linearized ODE for the time evolution of wall tension deviation

$$\begin{aligned}\frac{\mathrm{d}}{\mathrm{d}t}\Delta\sigma(t) &= \frac{\rho P}{R}\left[\frac{2r(t)}{M(t)}\dot{r}(t) - \frac{r^2(t)}{M^2(t)}\dot{M}(t)\right] \\ &\approx \left[\frac{1}{k_\mathrm{h}}\left[2\alpha - \frac{2k_\mathrm{g}r_\mathrm{h}^2\rho P}{RM_\mathrm{h}}\right] - \frac{k_\mathrm{g}\rho P r_\mathrm{h}^2}{RM_\mathrm{h}}\right]\Delta\sigma \\ &= [A + D]\Delta\sigma,\end{aligned} \tag{81}$$

which implies that stability criterion (73) also ensures the exponential stability for wall tension deviation, i.e.,

$$\lim_{t\to\infty} \Delta\sigma(t) = 0. \tag{82}$$

4.5 Summary of stability conclusions

When the following stability conditions are satisfied,

$$k_\mathrm{g} > \frac{\alpha R M_\mathrm{h}}{\rho P r_\mathrm{h}^2}\left[\frac{1}{1 + \frac{EM_\mathrm{h}}{2\rho P r_\mathrm{h}}}\right] \triangleq k_\mathrm{cr}, \quad \alpha > 0$$

the states $r(t)$, $M(t)$, $y(t)$ and $\sigma(t)$ for the nonlinear system (34–36) have the following stability behavior about the homeostatic states

$$\begin{aligned}&\|r(t)\| < \infty \Rightarrow r(t) \text{ is neutrally stable;} \\ &\|M(t)\| < \infty \Rightarrow M(t) \text{ is neutrally stable;} \\ &y(t) \to y_\mathrm{h} \Rightarrow y(t) \text{ is asymptotically stable;} \\ &\sigma(t) \to \sigma_\mathrm{h} \Rightarrow \sigma(t) \text{ is asymptotically stable,}\end{aligned} \tag{83}$$

Thus, stability analysis shows that even when the stability criterion (73) is satisfied, only σ and y will converge to corresponding homeostatic values, while M and r will only stay

bounded but not necessarily converge to the original homeostatic values. This matches observations in Baek et al. (2005), Wu and Shadden (2015) that in stable aneurysm expansion cases, only wall tension σ is able to recover the homeostatic value, while the geometry and mass density do not return to the original homeostatic states.

4.6 Extension to nonlinear constitutive relations

A linear constitutive relation for the vessel wall was considered above. Alternatively, we here assume a nonlinear Fung-type exponential constitutive relation, i.e., the strain energy density function is given by

$$\hat{W}(\lambda_{n(\tau)}(t)) = \frac{c_2}{4c_3}\left\{\exp\left[c_3\left(\lambda_{n(\tau)}(t)^2-1\right)^2\right]\right\}. \tag{84}$$

This type of constitutive relation is commonly used to describe the mechanical properties of vascular constituents (e.g., collagen and smooth muscle fibers). In the homeostatic state, the stretch ratio of the fiber, $\lambda_{n(\tau)}(t)$, is equal to G_h. Therefore, it can be represented as

$$\lambda_{n(\tau)}(t) = G_\mathrm{h} + \Delta\lambda, \tag{85}$$

where $\Delta\lambda$ is a small perturbation for the stretch ratio. Substituting the above equation into the nonlinear constitutive relation (84) yields

$$\begin{aligned}
&\hat{W}(\lambda_{n(\tau)}(t))\\
&= \frac{c_2}{4c_3}\left\{\exp\left[c_3\left([G_\mathrm{h}+\Delta\lambda]^2-1\right)^2\right]\right\}\\
&= \frac{c_2}{4c_3}\left\{\exp\left(c_3\left[G_\mathrm{h}^2-1\right]\right)-1\right\}\\
&\quad + c_2\exp\left(c_3\left[G_\mathrm{h}^2-1\right]\right)G_\mathrm{h}\left[G_\mathrm{h}^2-1\right]\Delta\lambda\\
&\quad + c_2\exp\left(c_3\left[G_\mathrm{h}^2-1\right]\right)G_\mathrm{h}^2(\Delta\lambda)^2+\mathcal{O}((\Delta\lambda)^3).
\end{aligned} \tag{86}$$

The relation between $\Delta\lambda$ and the strain in the fiber direction is

$$\Delta\lambda = \lambda_{n(\tau)}(t) - G_\mathrm{h} = (1+\epsilon) - G_\mathrm{h} = \epsilon - (G_\mathrm{h}-1), \tag{87}$$

where ϵ is the fiber strain. Using the above, we can rewrite the strain energy density function in terms of ϵ,

$$\begin{aligned}
\hat{W}(\lambda_{n(\tau)}(t)) \approx{}& \frac{c_2}{4c_3}\left\{\exp\left(c_3\left[G_\mathrm{h}^2-1\right]\right)-1\right\}\\
&+ c_2\exp\left(c_3\left[G_\mathrm{h}^2-1\right]\right)\\
&\times G_\mathrm{h}\left[G_\mathrm{h}^2-1\right](\epsilon-(G_\mathrm{h}-1))\\
&+ c_2\exp\left(c_3\left[G_\mathrm{h}^2-1\right]\right)\\
&\times G_\mathrm{h}^2(\epsilon-(G_\mathrm{h}-1))^2\\
={}& \Lambda_1 + R_0\epsilon + \frac{1}{2}E_\mathrm{tan}\epsilon^2,
\end{aligned} \tag{88}$$

where

$$\begin{aligned}
\Lambda_1 ={}& \frac{c_2}{4c_3}\left\{\exp(c_3[G_\mathrm{h}^2-1])-1\right\}\\
&+ c_2\left\{\exp(c_3[G_\mathrm{h}^2-1])-1\right\}G_\mathrm{h}(G_\mathrm{h}-1)^2,
\end{aligned} \tag{89}$$

$$\begin{aligned}
R_0 ={}& c_2\left\{\exp(c_3[G_\mathrm{h}^2-1])-1\right\}\\
&\times(-G_\mathrm{h}^3+G_\mathrm{h}^2-G_\mathrm{h}),
\end{aligned} \tag{90}$$

$$E_\mathrm{tan} = 2c_2\left\{\exp(c_3[G_\mathrm{h}^2-1])-1\right\}G_\mathrm{h}^2. \tag{91}$$

Substituting (88) into the force balance equation (16) yields

$$\begin{aligned}
Pr(t) &= R\frac{\partial W(t)}{\partial r(t)}\\
&= R\int_0^t \frac{m(\tau)}{\rho}q(t-\tau)\\
&\quad\times\left\{R_0\frac{\partial\epsilon}{\partial r(t)}+E_\mathrm{tan}\epsilon\frac{\partial\epsilon}{\partial r(t)}\right\}\mathrm{d}\tau\\
&= R\int_0^t \frac{m(\tau)}{\rho}q(t-\tau)\\
&\quad\times\left\{E_\mathrm{tan}\frac{G_\mathrm{h}^2}{r(\tau)^2}r(t)-(E_\mathrm{tan}-R_0)\frac{G_\mathrm{h}}{r(\tau)}\right\}\mathrm{d}\tau.
\end{aligned} \tag{92}$$

Taking time derivative of the above equation yields

$$\begin{aligned}
P\dot{r}(t) = R\Bigg\{&\frac{m(t)}{\rho}\left[E_\mathrm{tan}\frac{G_\mathrm{h}^2}{r(t)}-(E_\mathrm{tan}-R_0)\frac{G_\mathrm{h}}{r(t)}\right]\\
&+\int_0^t\frac{m(\tau)}{\rho}q(t-\tau)E_\mathrm{tan}\frac{G_\mathrm{h}^2}{r(\tau)^2}\dot{r}(t)\mathrm{d}\tau\\
&-\alpha\int_0^t\frac{m(\tau)}{\rho}q(t-\tau)\Bigg[E_\mathrm{tan}\frac{G_\mathrm{h}^2}{r(\tau)^2}r(t)\\
&-(E_\mathrm{tan}-R_0)\frac{G_\mathrm{h}}{r(\tau)}\Bigg]\mathrm{d}\tau\Bigg\}.
\end{aligned} \tag{93}$$

As before, if we define a similar extended state variable

$$y(t) = R\int_0^t\frac{m(\tau)}{\rho}q(t-\tau)E_\mathrm{tan}\frac{G_\mathrm{h}^2}{r(\tau)^2}\mathrm{d}\tau, \tag{94}$$

the differential equation for radius $r(t)$ can be obtained as

$$\begin{aligned}
\dot{r}(t) ={}& \frac{m(t)}{r(t)}\frac{RE_\mathrm{tan}\left[G_\mathrm{h}-\frac{E_\mathrm{tan}-R_0}{E_\mathrm{tan}}\right]G_\mathrm{h}}{P\rho}\\
&+\frac{1}{P}y(t)\dot{r}(t)-\alpha r(t),
\end{aligned} \tag{95}$$

which is similar to the differential equation for the linear material (32). After this, we can follow a parallel path to the stability analysis presented in the sections above and obtain a similar stabilizing criterion for nonlinear material

$$k_{\mathrm{g}} > \frac{\alpha R M_{\mathrm{h}}}{\rho P r_{\mathrm{h}}^2}\left[\frac{1}{1+\frac{E_{\tan} M_{\mathrm{h}}}{2\rho P r_{\mathrm{h}}}}\right] \triangleq k_{\mathrm{cr}}, \quad \alpha > 0.$$

Note that the effective difference between the stabilizing criteria for a linear material versus a nonlinear material comes by replacing the material stiffness E with $E_{\tan}$.

4.7 Extension to multiple component directions

Here we extend our framework from a single constituent model to a multiple constituent model where constituents are aligned in different directions. Assume that each constituent family is indexed by k and the angle between the constituent family direction and the circumferential directions is defined as $\alpha_k \in \left[\frac{-\pi}{2}, \frac{\pi}{2}\right]$. Since our model only considers the radial expansion of the vessel wall, we seek an effective stiffness caused by the multiple constituents. Assume the strain in the circumferential direction is ϵ. Due to the fact that all constituents deform together in a constrained mixture model, the strain in vascular constituent family k can be computed as

$$\begin{aligned}\epsilon_k &= \frac{\sqrt{(1+\epsilon)^2+\tan^2\alpha_k}-\sqrt{1+\tan^2\alpha_k}}{\sqrt{1+\tan^2\alpha_k}} \\ &= \frac{\epsilon}{1+\tan^2\alpha_k}+\mathcal{O}(\epsilon^2). \end{aligned} \tag{96}$$

The stress in the constituent family k can be computed as

$$\sigma_k = E\epsilon_k \approx \frac{E\epsilon}{1+\tan^2\alpha_k}, \tag{97}$$

Therefore, force in the vascular constituent family k is

$$f_k = A_k E \epsilon_k, \tag{98}$$

where A_k is the cross-section area of the constituent family k. We can represent the multiple constituents by an effective constituent in the circumferential direction by the following equivalency relation

$$\begin{aligned}\sum_k (A_k E\epsilon_k)\cos\alpha_k &= \sum_k f_k \cos\alpha_k \\ &= f = E_e\left(\sum_k A_k\right)\epsilon. \end{aligned} \tag{99}$$

Therefore, an effective stiffness E_e can be obtained as

$$E_e = \frac{\sum_k \frac{A_k\cos\alpha_k}{1+\tan^2\alpha_k}}{\sum_k A_k} E. \tag{100}$$

Because A_k is proportional to the mass density of each constituent family, M_k, the effective stiffness can be rewritten as

$$E_e = \frac{\sum_k \frac{M_k\cos\alpha_k}{1+\tan^2\alpha_k}}{\sum_k M_k} E. \tag{101}$$

After this point, we can apply the same formulas derived for the single constituent model and obtain similar stability conclusions.

5 Numerical experiments

The stability analysis and derived stability criterion presented above are, strictly speaking, applicable in the case of infinitesimal perturbations to the system. To understand how well these theoretical results hold in the context of large deviations, we must perform numerical integration of the original system. Therefore, in this section we simulate the vascular expansion based on the system of nonlinear differential equations (34–38). Material constants and geometric constants used in the simulations are listed in Table 1. All simulations were done within *Simulink*. In all simulations, pathological G&R is triggered by introducing 50 % initial uniform mass loss of vascular constituents as in Baek et al. (2005), Figueroa et al. (2009).

Based on the stabilizing criterion (73) and the given G&R parameters listed in Table 1, the critical value of the growth feedback constant is $k_{\mathrm{cr}} = 2.1 \times 10^{-6}$. The stabilizing condition (73) indicates that radial expansion is stable when $k_{\mathrm{g}} > k_{\mathrm{cr}}$, while the radial expansion is unstable when $k_{\mathrm{g}} \le k_{\mathrm{cr}}$. To test this, four scenarios of pathological G&R are simulated with different values of the growth feedback constant: Case (1) $k_{\mathrm{g}} = 1.5 \times 10^{-6}$, Case (2) $k_{\mathrm{g}} = 3.0 \times 10^{-6}$, Case (3) $k_{\mathrm{g}} = 5.0 \times 10^{-6}$ and Case (4) $k_{\mathrm{g}} = 7.0 \times 10^{-6}$. For these four cases, the time evolution of the state variables for vascular expansion, mass density $M(t)$, vessel radius $r(t)$, generalized stiffness $y(t)$ and wall tension $\sigma(t)$ were recorded and plotted in Fig. 2.

The simulation results show that when $k_{\mathrm{g}} > k_{\mathrm{cr}}$ (Cases 2–4), vascular expansion is stable. In these three stable cases, we observed that generalized stiffness $y(t)$ and wall tension $\sigma(t)$ converge to the corresponding homeostatic states asymptotically, while mass density $M(t)$ and vessel radius $r(t)$ only exhibit neutral stability, i.e., the values of the states remain bounded. In Case 1, where $k_{\mathrm{g}} < k_{\mathrm{cr}}$, vessel radius $r(t)$ and wall tension $\sigma(t)$ both increase unboundedly, which indicates unstable vascular expansion. Also observed

Table 1 Mechanical, geometric and G&R kinetic constants (Austin et al. 1989; Zeinali-Davarani et al. 2011)

$\alpha = 2.3$	$E = 1.9 \times 10^6$ Pa	$P = 13{,}332$ Pa	$r_h = 0.0075$ m
$G_h = 1.05$	$M_h = 1.0904\,\text{kg/m}^2$	$\sigma_h = 1.01 \times 10^5$ Pa	$\rho = 1050\,\text{kg/m}^3$

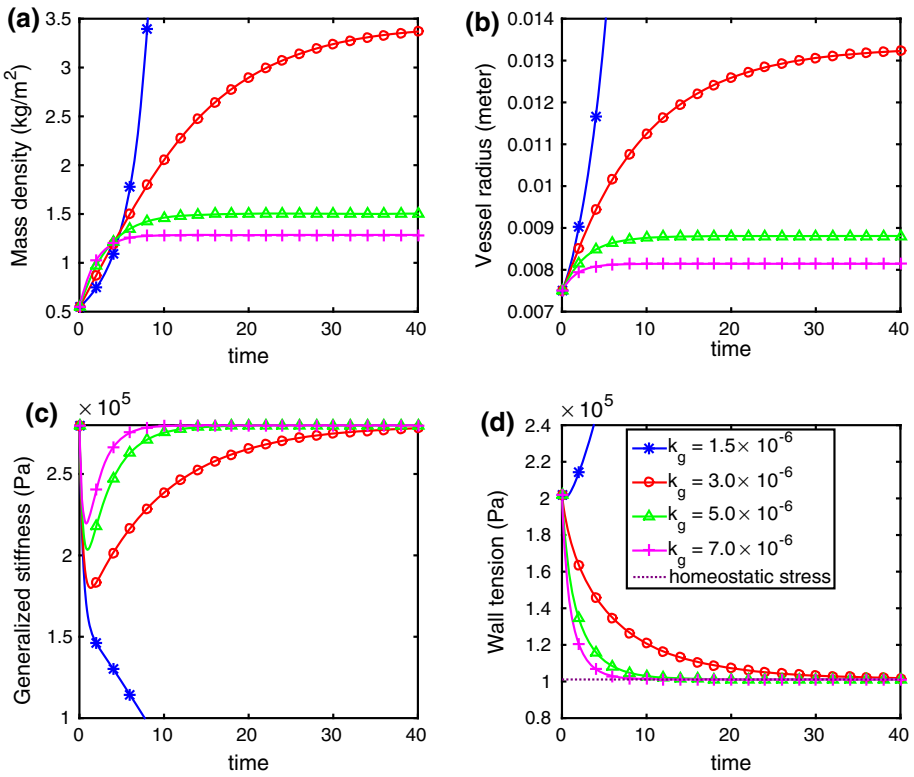

Fig. 2 Time evolution of vessel properties ($M(t)$, $r(t)$, $y(t)$ and $\sigma(t)$) using various values of growth feedback constant k_g from solving the nonlinear evolution equations. The corresponding critical value for the growth feedback constant is $k_{cr} = 2.1 \times 10^{-6}$

is that the larger the value of k_g, the faster the states converge to the steady states.

We also simulated four cases with increased stiffness E to study the influence of vessel stiffness on vascular expansion. The value of stiffness was increased to $E = 3.8 \times 10^6$ Pa, while all other parameters remained unchanged. For this value of E, the critical value for the growth feedback constant is $k_{cr} = 1.0 \times 10^{-6}$. Four scenarios were considered, with Case (1) $k_g = 1.5 \times 10^{-6}$, Case (2) $k_g = 3.0 \times 10^{-6}$, Case (3) $k_g = 5.0 \times 10^{-6}$ and Case (4) $k_g = 7.0 \times 10^{-6}$, and the time course of the four state variables is plotted in Fig. 3. For the elevated value of stiffness E, all four cases satisfy the stabilizing condition $k_g > k_{cr}$ and all four cases obtain stable vascular expansion, including the case of $k_g = 1.5 \times 10^{-6}$ that was unstable for the normal value of stiffness E.

Lastly, we simulated four cases considering an increase in vascular constituent decay constant $\alpha = 4.6$. This corresponds to an increase in turnover rate of vascular constituents, e.g., collagen and smooth muscle. For this scenario, the critical value for the growth feedback constant was $k_{cr} = 4.1 \times 10^{-6}$. The time evolution of the four state variables for Case (1) $k_g = 1.5 \times 10^{-6}$, Case (2) $k_g = 3.0 \times 10^{-6}$, Case (3) $k_g = 5.0 \times 10^{-6}$ and Case (4) $k_g = 7.0 \times 10^{-6}$ is plotted in Fig. 4. With the elevated value of the decay constant, Cases (3) and (4) satisfy the stabilizing criterion, while Cases (1) and (2) do not. Figure 4 shows that only in Cases (3) and (4), vessel radius remains bounded and wall tension converges to the homeostatic value, while in Cases (1) and (2) G&R results in unbounded vascular expansion. Case (2), which is stable under the normal conditions, is destabilized due to elevated decay constant α.

6 Discussion

While prior works (Figueroa et al. 2009; Aparício et al. 2014; Sheidaei et al. 2011; Wu and Shadden 2015) have focused on computationally investigating vascular expansion based on the constrained mixture theory of vascular G&R, we herein provide an analytical study of the stability properties of this model. Under appropriate assumptions, the constrained mixture model was used to develop a nonlinear ODE system governing vascular growth, and stability criterion (73) were derived for growth about the homeostatic state in terms of

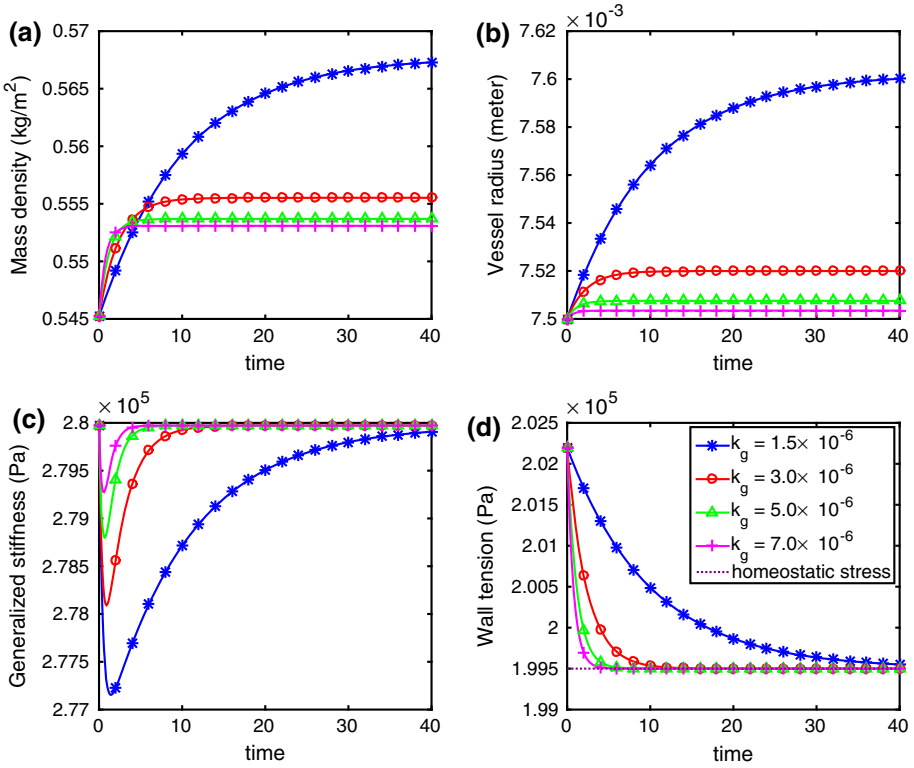

Fig. 3 Time evolution of vessel properties ($M(t)$, $r(t)$, $y(t)$ and $\sigma(t)$) using various values of growth feedback constant k_g for increased arterial stiffness **E**. The corresponding critical value for the growth feedback constant is $k_{cr} = 1.0 \times 10^{-6}$

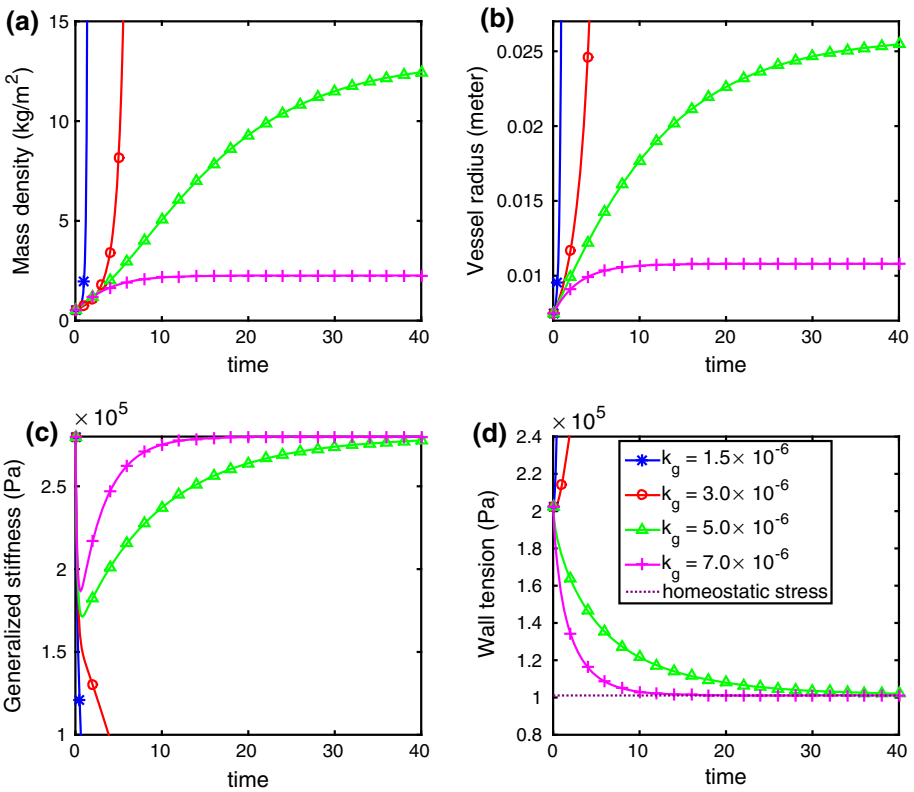

Fig. 4 Time evolution of vessel properties ($M(t)$, $r(t)$, $y(t)$ and $\sigma(t)$) using various values of growth feedback constant k_g for increased decay constant α. The corresponding critical value for the growth feedback constant is $k_{cr} = 4.1 \times 10^{-6}$

G&R kinetic parameters, geometric quantities and material properties.

To obtain stability conclusions for the nonlinear system about the homeostatic state, we first linearized the nonlinear equations. The resulting linearization was shown to be degenerate, failing to determine the stability of the original nonlinear system. Indeed, the neutral stability property of vascular G&R observed in prior theoretical (Cyron and Humphrey 2014; Cyron et al. 2014) and computational (Wu and Shadden 2015) studies is due to this degeneracy; however, stability properties for the original (nonlinear) system had not previously been clarified. To address this problem, we consider the two-state subsystem $(\Delta M, \Delta y)$, in which Δr was eliminate due to its linear dependence on ΔM. While the resulting equation for ΔM was non-homogenous, it was homogenized by taking its time derivative. The resulting dynamics for $(\Delta \dot{M}, \Delta y)$ were made exponentially stable by requiring the eigenvalues to be negative, by which local exponential stability of the mass density rate $\Delta \dot{M}$ and generalized stiffness Δy for the nonlinear system were established. Using the local exponential stability of $\Delta \dot{M}$ and the triangle inequality, neutral stability of the mass density $M(t)$ for the nonlinear system was established. Similar arguments imply that the vessel radius $r(t)$ is neutrally stable and wall tension $\sigma(t)$ is exponentially stable for the nonlinear system.

When converting the integral equation (21) for the vessel radius r to a non-delayed ODE, we derived an extended state y defined by (31). The meaning of y is discussed here. Consider the vascular force in the circumferential direction

$$\begin{aligned} T_\theta(t) &= Pr(t) \\ &= R\int_0^t \frac{m(\tau)}{\rho} q(t-\tau) E\left[G_\mathrm{h}\frac{r(t)}{r(\tau)} - 1\right]\frac{G_\mathrm{h}}{r(\tau)}\mathrm{d}\tau. \end{aligned} \tag{102}$$

Now take the first variation of the above equation corresponding to a snapshot of the G&R process. Since $q(t)$ is a known function of t and time is fixed when taking the variation, δq and δt are both equal to zero. The only two functions that have nonzero first variation are δT_θ and δr, and therefore, the equation is reduced into the following form

$$\begin{aligned} \delta T_\theta &= \delta\left[R\int_0^t \frac{m(\tau)}{\rho} q(t-\tau) \right. \\ &\quad \left. \times E\left[G_\mathrm{h}\frac{r(t)}{r(\tau)} - 1\right]\frac{G_\mathrm{h}}{r(\tau)}\mathrm{d}\tau\right] \\ &= R\int_0^t \frac{m(\tau)}{\rho} q(t-\tau) \\ &\quad \times E\delta\left[G_\mathrm{h}\frac{r(t)}{r(\tau)} - 1\right]\frac{G_\mathrm{h}}{r(\tau)}\mathrm{d}\tau \\ &= R\int_0^t \frac{m(\tau)}{\rho} q(t-\tau) \\ &\quad \times E\frac{G_\mathrm{h}^2}{r^2(\tau)}\mathrm{d}\tau \cdot \delta r \\ &= y(t)\cdot\delta r. \end{aligned} \tag{103}$$

Therefore, the extended state y can be defined as the ratio of variations of stress and strain in circumferential direction, multiplied by a constant $\frac{R}{h}$,

$$y = \frac{\delta T_\theta}{\delta r} = \frac{\delta T_\theta / h}{\delta r / R}\frac{R}{h} = \frac{\delta \sigma_\theta}{\delta \epsilon_\theta}\frac{R}{h}. \tag{104}$$

This implies that y physically represents a generalized stiffness resisting radial expansion for the mixture of vascular constituents. In our study, we only consider one species of vascular constituents aligned in the circumferential direction for simplicity of exposition. However, we note that within one constituent family, constituents produced at different times τ form a *mixture* of constituents that possess different natural configurations. We demonstrated in Sect. 4.7 that it is straightforward to extend the theory to a mixture model with multiple species in the current setting; however, cases of asymmetric expansion would require more involved analysis of the associated kinematics.

The derived stability criterion for the nonlinear system were verified by numerical simulations. As shown in Fig. 2, for the three cases (Cases 2–4) satisfying the derived stability criteria, only the generalized stiffness y and the wall tension σ converge to their homeostatic values, while vessel radius r and mass density M only remain bounded (they do not converge to specific homeostatic values). These results from numerically integrating the nonlinear evolution equations are consistent with the stability conclusions obtained from the presented theoretical analysis. When the system is stable, only y and σ exhibit local exponential stability, while r and M exhibit neutral stability. It is interesting to note that these convergence behaviors match with prior observations from computational studies in idealized (Baek et al. 2005, 2006) and patient-specific (Wu and Shadden 2015) geometries, where less restrictive modeling assumptions were employed than those used to develop the theoretical model herein. Moreover, we note that while the theoretical analysis only implies *local* stability properties about the homeostatic state, the numerical experiments considered *large* deviations from the homeostatic state; nonetheless, identical stability properties were observed as predicted by the theoretical model.

For the numerical experiments, pathological G&R was triggered by introducing an initial mass loss to the vessel wall. This caused an immediate weakening of vessel, as reflected in the initial drop of the generalized stiffness y (see Fig. 2c). However, for the three stable cases (Cases 2–4), after the initial drop due to mass loss, the generalized stiffness y recovered back to the homeostatic value. This is because when $k_\mathrm{g} > k_\mathrm{cr}$, thickening of vessel wall caused

by stress-mediated growth is fast enough to compensate the natural expansion caused by the initial mass loss and natural turnover of vascular constituent. On the other hand, for Case 1, $k_g \leq k_{cr}$, and the stress-mediated growth (feedback) is not strong enough to compensate for the weakening of the vessel and natural turnover. Therefore, expansion proceeds with continuous increase in vessel radius r and wall tension σ.

Based on the stabilizing criterion (73), the stability of vascular expansion depends on growth parameters (k_g, α) and material properties ($\mathbf{E}$, ρ). To understand how these factors influence the stability behavior, we first increased the material stiffness E holding all other parameters at their nominal values. The simulation results (Fig. 3) show that, when stiffness $\mathbf{E}$ is doubled, all four values of the feedback growth constant k_g are stable, including the case $k_g = 1.5 \times 10^{-6}$, which was originally not stable. This can be seen from the definition of the critical value k_{cr}

$$k_{cr} \triangleq \frac{\alpha R M_h}{\rho P r_h^2}\left[\frac{1}{1+\frac{E M_h}{2\rho P r_h}}\right]. \tag{105}$$

When material stiffness E increases, k_{cr} decreases and stabilizing criterion will be easier to satisfy. This result, that increased arterial stiffness may have a stabilizing effect, matches observations in Cyron et al. (2014), Satha et al. (2014). We note, however, that in previous clinical studies (Dijk et al. 2004; Safar et al. 2014), it has been observed that increased wall stiffness correlates with the occurrence of aortic aneurysm. However, increased vessel wall stiffness may be a consequence of the disease than a direct cause. Alternatively, other factors such as multidirectional expansion and biochemical effects may be at play in vivo that are not considered in the present modeling.

of $k_g = 1.5 \times 10^{-6}$ and $k_g = 3.0 \times 10^{-6}$ fail to satisfy the stabilizing condition. Prior studies (Satta et al. 1995; Abdul-Hussien et al. 2007) have observed increased collagen turnover in abdominal aortic aneurysms and ruptured abdominal aortic aneurysms. Additionally, Etminan et al. (2014) found that the collagen turnover is significantly more rapid in patients with risk factors for aneurysm formation/rupture, such as smoking or hypertension. These observations are consistent with the theoretical and computational analyses here that increased decay constant α can destabilize the vascular G&R process.

While we assumed (mean) blood pressure to be constant in our analysis, we here consider the effect of increased blood pressure (hypertension) on the stability of vascular G&R. Based on the stabilizing criterion (105), an increase in mean blood pressure P will cause a decrease in the critical value k_{cr}, which indicates that hypertension acts as a stabilizing factor. However, this is inconsistent with evidence that hypertension is a risk factor for aneurysm growth and rupture (Choke et al. 2005). It is important to notice that (40) holds true only when P denotes the pressure producing the homeostatic hoop stress σ_h when $M = M_h$ and $r = r_h$. Let us denote the homeostatic pressure as P_h. In order to study the influence of mean blood pressure on the stability of vascular expansion, we need to consider a deviation from the homeostatic pressure. Thus, for a general pressure P in (21), we assume

$$P = P_h + \Delta P \tag{106}$$

where ΔP is a small pressure deviation and $P_h = \frac{E[G_h - 1]M_h}{\rho r_h}$ based on (40). Note that we here only consider a constant change of pressure, i.e., ΔP is independent of time. After the same procedure of linearization, the three-state linear system equation becomes

$$\frac{\mathrm{d}}{\mathrm{d}t}\begin{bmatrix}\Delta r\\ \Delta M\\ \Delta y\end{bmatrix} = \begin{bmatrix} \frac{1}{k_h}\left[\alpha - \frac{k_g \rho P_h r_h^2}{R M_h}\right]\left[2\Delta r - \frac{r_h}{M_h}\Delta M + \frac{r_h}{P_h}\Delta P\right] \\ \frac{k_g \rho P_h r_h}{R}\left[2\Delta r - \frac{r_h}{M_h}\Delta M + \frac{r_h}{P_h}\Delta P\right] \\ -\frac{k_2 M_h}{r_h^3}\left[\alpha - \frac{k_g \rho P_h r_h^2}{R M_h}\right]\left[2\Delta r - \frac{r_h}{M_h}\Delta M + \frac{r_h}{P_h}\Delta P\right] - \alpha\left[\Delta y - \frac{k_2 M_h}{r_h^2 P_h}\Delta P\right] \end{bmatrix} \tag{107}$$

We also sought to understand the influence of growth parameters (k_g, α). The constant α defines the rate of vascular constituent turnover. When α was increased, the results in Fig. 4 demonstrate a destabilizing behavior. Namely, Case 2 ($k_g = 3.0 \times 10^{-6}$) that was stable for the nominal parameter set led to unstable expansion. Again, this trend can be anticipate from (105). As α is increased, the critical value for the feedback growth constant also increases, and the cases

If we set the new deviation variable for generalized stiffness $y(t)$ as

$$\overline{\Delta y} \triangleq \Delta y - \frac{k_2 M_h}{r_h^2 P_h}\Delta P, \tag{108}$$

a similar two-state homogeneous system can be obtained with respect to $(\Delta\dot{M}, \overline{\Delta y})$ by making use of the same linear relation (66)

$$\frac{\mathrm{d}}{\mathrm{d}t}\begin{bmatrix}\dot{\Delta M}\\ \dot{\Delta y}\end{bmatrix}=\begin{bmatrix}\frac{k_g\rho P_h r_h}{R}\left[2B_1-\frac{r_h}{M_h}\right] & 0\\ B_3 & -\alpha\end{bmatrix}\begin{bmatrix}\dot{\Delta M}\\ \dot{\Delta y}\end{bmatrix}. \tag{109}$$

Note that the coefficient matrix of the above two-state system is the same as that of (70), except the pressure P is now replaced by the homeostatic pressure P_h. Therefore, the same stabilizing condition is obtained as follows

$$k_g > \frac{\alpha R M_h}{\rho P_h r_h^2}\left[\frac{1}{1+\frac{EM_h}{2\rho P_h r_h}}\right] \triangleq k_{cr}, \quad \alpha > 0. \tag{110}$$

Substituting $P_h = \frac{E[G_h-1]M_h}{\rho r_h}$ into the above inequality yields

$$k_{cr} = \frac{\alpha}{EG_h\left[G_h-\frac{1}{2}\right]} \approx 1.732\frac{\alpha}{E} \tag{111}$$

which is independent of the pressure deviation ΔP. Therefore, from the linear analysis, the stability of vascular G&R is independent of mean blood pressure.

However, the above equation does not imply that blood pressure does not affect solution behavior. Note that $B_1 > 0$ if

$$k_g < \frac{\alpha R M_h}{\rho P r_h^2} = \frac{\alpha}{EG_h\left[G_h-1\right]} \approx 19.048\frac{\alpha}{E} \gg k_{cr}. \tag{112}$$

We here assume the normal range of the value for k_g is around k_{cr}, which is much less than $19.048\frac{\alpha}{E}$. Therefore, B_1 is always positive. Based on the linear relation between $\Delta r(t)$ and $\Delta M(t)$ in (66), and the second equation of (107),

$$\frac{\mathrm{d}}{\mathrm{d}t}\Delta M = \lambda_1 \Delta M + \frac{k_g\rho P_h r_h}{R}\left[2B_2+\frac{r_h}{P_h}\Delta P\right], \tag{113}$$

where

$$\begin{aligned}\lambda_1 &= \frac{k_g\rho P_h r_h}{R}\left[2B_1-\frac{r_h}{M_h}\right]\\ &= 2EG_h\left[G_h-1\right]\left[G_h-\frac{1}{2}\right]\left[k_{cr}-k_g\right].\end{aligned} \tag{114}$$

The solution to the above equation is

$$\Delta M(t) = B_4 e^{\lambda_1 t} + \frac{k_g\rho P_h r_h}{-\lambda_1 R}\left[2B_2+\frac{r_h}{P_h}\Delta P\right], \tag{115}$$

where B_4 is a constant that depends on the initial condition. Based on the linear relation (66), the solution for radius change $\Delta r(t)$ is

$$\begin{aligned}\Delta r(t) &= B_1 B_4 e^{\lambda_1 t}\\ &\quad + \frac{B_1 k_g\rho P_h r_h}{-\lambda_1 R}\left[2B_2+\frac{r_h}{P_h}\Delta P\right]+B_2.\end{aligned} \tag{116}$$

The stability of the solution is determined by the exponential term $e^{\lambda_1 t}$. Since ΔP does not influence λ_1, it does not influence the stability of the system. However, ΔP does influence the particular solutions for $\Delta M(t)$ and $\Delta r(t)$. Therefore, ΔP will cause a shift of the steady states (if they exist), but not the stability of the system.

In the case of stable vascular G&R ($k_g > k_{cr}$, $\lambda_1 < 0$),

$$\Delta M(t\to+\infty) = \frac{k_g\rho P_h r_h}{-\lambda_1 R}\left[2B_2+\frac{r_h}{P_h}\Delta P\right], \tag{117}$$

$$\Delta r(t\to+\infty) = \frac{B_1 k_g\rho P_h r_h}{-\lambda_1 R}\left[2B_2+\frac{r_h}{P_h}\Delta P\right]+B_2. \tag{118}$$

Therefore, if ΔP increases, it will cause the final mass density to increase. Indeed, vascular mass density needs to increase in order to balance the increased pressure and maintain the homeostatic stress σ_h. Also (108) shows that increased ΔP causes an increased shift of Δy. This also corresponds to the fact that the overall stiffness of the vascular mixture needs to increase to compensate for the increased pressure. Similarly, due to the positiveness of B_1, increased ΔP will cause the increased shift of the final steady state radius. In comparison with prior studies, it has similarly been shown that hypertension (i.e., increased ΔP) does not change the stability of expansion; however, it does increase the thickness (proportional to mass density) of vessel wall (Wolinsky 1972; Bots et al. 1993) and the final size of the aneurysm. Also based on the first equation of (107), hypertension increases the vessel expansion rate $\dot{\Delta r}$, which is consistent with prior clinical findings (Huang et al. 2008), regardless of whether the expansion is stable or not. The analysis above considers only the direct influence of hypertension on stability of vascular G&R. However, hypertension may change stability through other factors not considered here. For example, Nissen et al. (1978) indicate that collagen turnover in aorta and arteries are increased under hypertension. This corresponds to increased α in our analysis, which is a destabilizing factor for vascular G&R.

7 Conclusion

A theoretical study of the stability properties of vascular G&R was presented. A system of nonlinear ordinary differential equations was obtained from the integral equations of the constrained mixture theory for G&R. Degeneracy of the linearized state equations about the homeostatic state results in a "neutral stability property" for vascular growth and remodeling previously observed in prior computational studies, and renders linear stability analysis inconclusive. To resolve this problem and extend the stability conclusions to the original nonlinear system, we were able to construct a two-state

sub-system to apply Lyapunov's indirect method. Based on stability analysis for the nonlinear system, we derived a stabilizing condition for radial expansion in terms of material properties (E, ρ), G&R parameters (k_g, α) and geometry (R, r_h). The neutral stability shows that, in the stable expansion case, only wall tension σ and generalized stiffness y exhibit convergence to the corresponding homeostatic values, while vessel radius r and mass density of vascular constituents only remain bounded without converging to any specific values. The derived theoretical stability criterion was demonstrated to hold broadly in numerical studies were deviations from the homeostatic state were large. Additionally, we studied the effect of increased stiffness E and increased decay constant α on the stability of radial expansion. Both the theoretical analysis and numerical simulations showed that increased stiffness has a stabilizing effect of vascular expansion, while an increased turnover rate of vascular constituents has a destabilizing effect. Finally, the effect of hypertension on the stabilizing criterion was studied. This analysis showed that while increased blood pressure may cause a shift of the final steady states, it does not influence the stability properties of the model.

References

Abdul-Hussien H, Soekhoe R, Weber E, Jan H, Kleemann R, Mulder A, Van Bockel J, Hanemaaijer R, Lindeman J (2007) Collagen degradation in the abdominal aneurysm: a conspiracy of matrix metalloproteinase and cysteine collagenases. Am J Pathol 170(3):809–817

Aparício P, Mandaltsi A, Boamah J, Chen H, Selimovic A, Bratby M, Uberoi R, Ventikos Y, Watton P (2014) Modelling the influence of endothelial heterogeneity on the progression of arterial disease: Application to abdominal aortic aneurysm evolution. Int J Numer Methods Biomed Eng 30(5):563–586

Austin G, Schievink W, Williams R (1989) Controlled pressure–volume factors in the enlargement of intracranial aneurysms. Neurosurgery 24(5):722–730

Baek S, Rajagopal K, Humphrey J (2005) Competition between radial expansion and thickening in the enlargement of an intracranial saccular aneurysm. J Elast 80(1–3):13–31

Baek S, Rajagopal K, Humphrey J (2006) A theoretical model of enlarging intracranial fusiform aneurysms. J Biomech Eng 128(1):142–149

Bogen D, McMahon T (1979) Do cardiac aneurysms blow out? Biophys J 27(2):301

Bots M, Hofman A, de Bruyn A, De Jong P, Grobbee D (1993) Isolated systolic hypertension and vessel wall thickness of the carotid artery. The Rotterdam Elderly Study. Arterioscler Thromb Vasc Biol 13(1):64–69

Choke E, Cockerill G, Wilson W, Sayed S, Dawson J, Loftus I, Thompson M (2005) A review of biological factors implicated in abdominal aortic aneurysm rupture. Eur J Vasc Endovasc Surg 30(3):227–244

Cyron C, Humphrey J (2014) Vascular homeostasis and the concept of mechanobiological stability. Int J Eng Sci 85:203–223

Cyron C, Wilson J, Humphrey J (2014) Mechanobiological stability: a new paradigm to understand the enlargement of aneurysms? J R Soc Interface 11(100):20140680

Dijk J, Van Der Graaf Y, Grobbee D, Banga J, Bots M et al (2004) Increased arterial stiffness is independently related to cerebrovascular disease and aneurysms of the abdominal aorta the second manifestations of arterial disease (smart) study. Stroke 35(7):1642–1646

Etminan N, Dreier R, Buchholz B, Beseoglu K, Bruckner P, Matzenauer C, Torner J, Brown R, Steiger H, Hänggi D et al (2014) Age of collagen in intracranial saccular aneurysms. Stroke 45(6):1757–1763

Figueroa A, Baek S, Taylor C, Humphrey J (2009) A computational framework for fluid–solid-growth modeling in cardiovascular simulations. Comput Methods Appl Mech Eng 198(45):3583–3602

Holzapfel G, Gasser T, Ogden R (2000) A new constitutive framework for arterial wall mechanics and a comparative study of material models. J Elast Phys Sci Solids 61(1–3):1–48

Huang Y, Gloviczki P, Duncan A, Kalra M, Hoskin T, Oderich G, McKusick M, Bower T (2008) Common iliac artery aneurysm: expansion rate and results of open surgical and endovascular repair. J Vasc Surg 47(6):1203–1211

Humphrey J (2006) Towards a theory of vascular growth and remodeling. In: Holzapfel G, Ogden R (eds) Mechanics of biological tissue. Springer, Berlin, pp 3–15. doi:10.1007/3-540-31184-X_1

Humphrey J (2013) Cardiovascular solid mechanics: cells, tissues, and organs. Springer, New York

Humphrey J, Rajagopal K (2002) A constrained mixture model for growth and remodeling of soft tissues. Mathematical Models and Methods in Applied Sciences 12(03):407–430

Nissen R, Cardinale G, Udenfriend S (1978) Increased turnover of arterial collagen in hypertensive rats. Proc Natl Acad Sci 75(1):451–453

Safar M, O'Rourke M, Frohlich E (2014) Blood pressure and arterial wall mechanics in cardiovascular diseases. Springer, Berlin

Satha G, Lindström S, Klarbring A (2014) A goal function approach to remodeling of arteries uncovers mechanisms for growth instability. Biomech Model Mechanobiol 13(6):1243–1259

Satta J, Juvonen T, Haukipuro K, Juvonen M, Kairaluoma M (1995) Increased turnover of collagen in abdominal aortic aneurysms, demonstrated by measuring the concentration of the aminoterminal propeptide of type iii procollagen in peripheral and aortal blood samples. J Vasc Surg 22(2):155–160

Sheidaei A, Hunley S, Zeinali-Davarani S, Raguin L, Baek S (2011) Simulation of abdominal aortic aneurysm growth with updating hemodynamic loads using a realistic geometry. Med Eng Phys 33(1):80–88

Valentin A, Humphrey J (2009) Evaluation of fundamental hypotheses underlying constrained mixture models of arterial growth and remodelling. Philos Trans R Soc Lond A Math Phys Eng Sci 367(1902):3585–3606

Verhulst F (1996) Nonlinear differential equations and dynamical systems. Springer, Berlin

Watton P, Raberger N, Holzapfel G, Ventikos Y (2009) Coupling the hemodynamic environment to the evolution of cerebral aneurysms: computational framework and numerical examples. J Biomech Eng 131(10):101003

Wolinsky H (1972) Long-term effects of hypertension on the rat aortic wall and their relation to concurrent aging changes: morphological and chemical studies. Circ Res 30(3):301–309

Wu J, Shadden S (2015) Coupled simulation of hemodynamics and vascular growth and remodeling in a subject-specific geometry. Ann Biomed Eng 43(7):1543–1554

Zeinali-Davarani S, Sheidaei A, Baek S (2011) A finite element model of stress-mediated vascular adaptation: application to abdominal aortic aneurysms. Comput Methods Biomech Biomed Eng 14(9):803–817